High performance shape memory effect in nitinol wire for actuators with increased operating temperature range

Riccardo Casati*,‡, Carlo Alberto Biffi†, Maurizio Vedani* and Ausonio Tuissi†
*Department of Mechanical Engineering, Politecnico di Milano
Via La Masa 1, Milano 20143, Italy

†CNR-IENI, National Research Council of Italy — Institute for Energetics and Interphases, Corso Promessi Sposi 29
Lecco 23900, Italy

‡riccardo.casati@polimi.it

Received 8 June 2014; Accepted 23 June 2014; Published 11 July 2014

Shape memory alloys (SMAs) can recover high deformation values by means of a diffusionless, reversible, solid-state martensitic transformation (MT) that takes place between two stable phases: the austenite and the martensite.[1–4] SMAs have been commonly classified into two well distinct classes according to their thermodynamically stable phase in absence of load at environmental temperature:

(i) the martensitic SMAs showing the so-called shape memory effect (SME) which are mainly employed for actuator devices[5–10] and
(ii) the austenitic SMAs showing the pseudoelastic or superelastic effect (SE) which are widely used in biomedical field, for instance they are employed for vascular stents, or for damping applications.[11–16]

The intermetallic NiTi (also known as Nitinol) is the most used SMA, thanks to its excellent fatigue and functional properties, biocompatibility, relatively good ductility and low cost. Phase transition temperatures can be controlled through the Ni-content. Ni-rich alloys exhibit austenitic phase at room temperature (RT) and they are commonly employed in applications requiring the SE. When Ni content in NiTi is lower than 50.4 at.% and especially when the alloy is Ti-rich, the martensitic phase is exhibited at RT and the SME is exploited for actuator applications.[5–10,17]

Recently, Ni-rich Nitinol wires, with fully austenitic phase at RT, were used for the description of a new phenomenon named high performance shape memory effect (HP-SME).[4] It consists in the thermal cycling of stress induced martensite (SIM) and it allows achieving extremely high mechanical work (stresses of the order of 1 GPa), higher than that produced by conventional shape memory actuators based on the heating/cooling of detwinned martensite. In particular, when loading the austenite phase above a critical stress, SIM is induced and the material deformation proceeds at almost constant stress. As the SIM is heated above the austenite finish temperature (A_f) under constant applied force, it shrinks back due to the stabilization of the parent phase and the macroscopic deformation is therefore recovered. Finally, as the material is cooled to the RT, a complete SIM state is reproduced and the deformation is restored.[4]

In Ref. 4, wires showing austenitic structure at RT were used so as to obtain functioning temperatures under load suitable for RT shape memory actuator. On the contrary, in this work, the principle of HP-SME is exploited by martensitic NiTi micro-wires with A_f higher than RT. The wires were heated upon A_f, then loaded above the superelastic plateau to induce SIM and thermally cycled between 80°C and 180°C. According to this strategy, martensitic NiTi SMA are proposed in this study to be used in a temperature range higher than A_f as suitable materials for warm-temperature actuators. SMAs with transformation temperature higher than 120°C are generally named high-temperature SMAs.[18] Such high characteristic temperatures are achieved by adding a third alloying element to the NiTi system, such as Pt or Pd with a significant increase of costs.[19,20] Other high-temperature SMAs, for instance CuZr-based alloys, have also been studied but they showed poor workability and thermal stability.[21,22] In this work, martensitic NiTi is proposed as suitable material capable of working in a warm temperature range, higher than that proposed by NiTi manufacturers and close to the operating range of high-temperature SMAs.

NiTi wire of diameter 150 μm (Flexinol®) was used for the experiments. The transformation temperatures of the intermetallic compound were measured by differential scanning calorimeter (DSC, Seiko 220C) with a scanning rate of 10°C*min^{-1}. Tensile stress/strain tests and thermal loops under constant stress were both performed by dynamical mechanical thermal analyzer (DMTA, TA Instrument Q800) equipped with tension clamp for uniaxial tests. The heating/cooling rate was 2°C*min^{-1}. Functional fatigue tests were carried out at 80°C, by an experimental apparatus, placed in a thermostatic chamber (Angelantoni Sunrise 250). Wires of 100 mm in length were vertically positioned and constrained to the system structure by an upper clamp. For inducing a complete SIM state, the samples were axially loaded (600 MPa) by a weight that was fixed to a lower clamp. A National Instrument Labview program controlled a power source connected to the clamps to heat the wire by square electrical pulse (Joule effect). This program allowed a fast control mode of the wire deformation: the current was switched off when the sample recovered a strain value of 3% to avoid overheating of the wire. The cooling time was fixed to 5 s. The displacement was measured by a linear voltage differential transducer (LVDT, Macro Sensors HSTA 750–125). Details of the cycling apparatus are reported elsewhere.[22,23]

Figure 1 shows the results of calorimetric analysis carried out on the as received wire. It exhibits a single-stage inverse transformation (Martensite B19' → Austenite B2) and a two-stage direct transformation (Austenite B2 → R-phase → Martensite B19'). The wire shows an A_f temperature higher than 70°C. Thus, a temperature of 80°C was chosen for the further tests in order to operate with fully austenitic structure wires.

Tensile tests were performed to evaluate the stress level of the superelastic plateau (Fig. 2). As expected, at 80°C the material shows the conventional superelastic behavior (flag like stress/strain loops) of a SM material loaded in the austenitic phase above A_f. Since the commercial wire used for

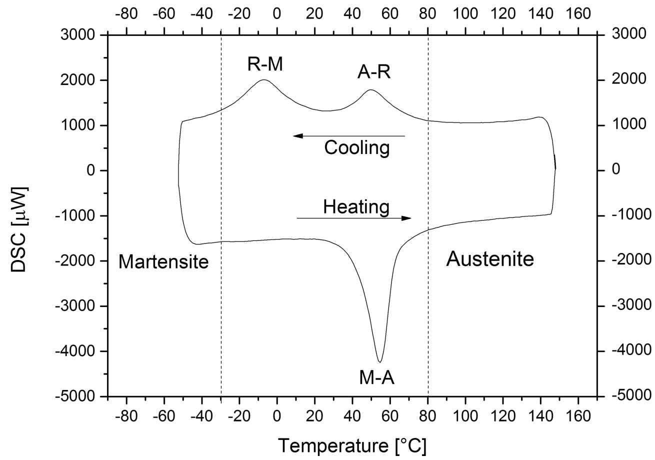

Fig. 1. DSC curve of the NiTi wire (M = martensite, A = austenite, R = R-phase). It is worth noting that no load is applied to the sample.

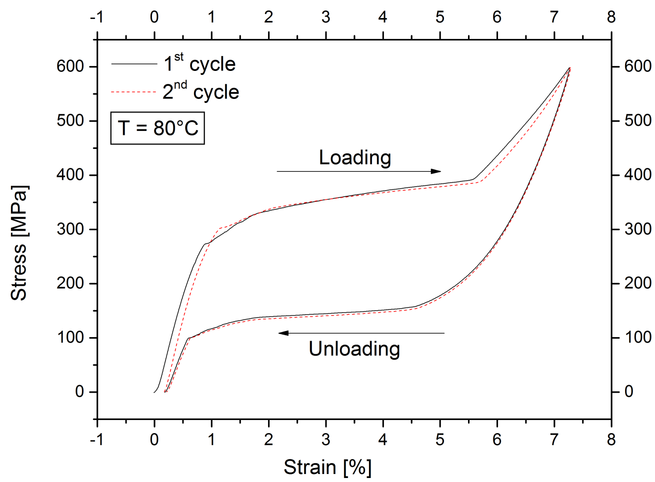

Fig. 2. Tensile curve at 80°C of the NiTi wire.

this work is not optimized for superelastic applications, the cycling response of the material is affected by mechanical loading/unloading. However, starting from the second cycle, the wire shows an almost complete strain recovery with a permanent strain $< 0.04\%$ upon unloading. The end of the transformation plateau occurs at about 400 MPa, so the martensite is completely induced at 80°C by applying external loads exceeding this stress threshold.

The results obtained from quasi-static thermal loop under constant stress (600 MPa) are depicted in Fig. 3. The austenitic wire was axially loaded at 80°C up to 600 MPa, above the superelastic plateau required to induce the SIM. Then, it was heated up to 180°C, under constant stress of 600 MPa and a deformation of 5.5% was recovered during the transformation from SIM to austenite. Finally, the wire was cooled down to 80°C, keeping the applied constant stress of 600 MPa, and the deformation was restored due to the release of SIM as the temperature decreased. The material showed a

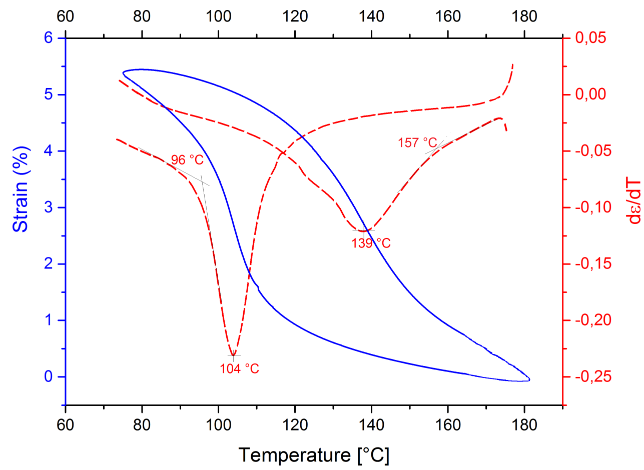

Fig. 3. Strain-temperature curve: thermal loop, between 80°C and 180°C, under constant stress of 600 MPa.

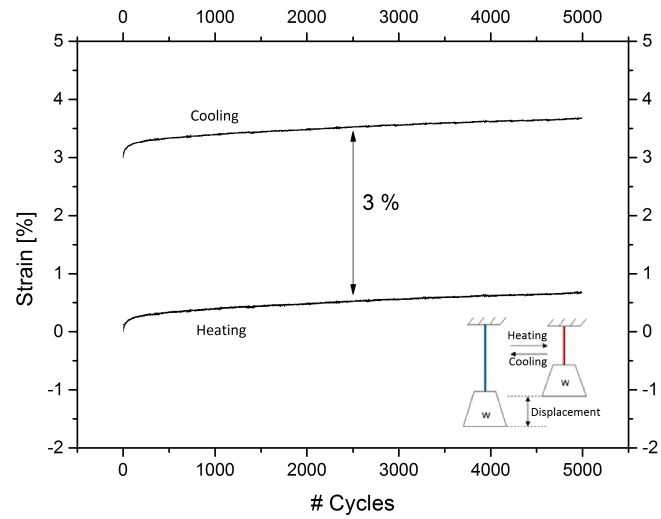

Fig. 4. Fatigue test performed on Ni49Ti51 at 80°C under constant stress of 600 MPa.

complete HP-SME within a temperature range of 80–180°C. The first derivative of the T–ε curve branches ($d\varepsilon/dT$) has been added to the graph to highlight the characteristic temperatures of the material. The SMA wire shows a relatively narrow thermal hysteresis between the heating and the cooling branch of the curve. The difference in temperature measured at the peaks of the derivative $d\varepsilon/dT$ curves, which correspond to the inflection points of the T–ε curve is about 35°C. However, the applied/recovered strain turned out to be rather broadened in the temperature range; the transformation do not indeed occur sharply. Under 600 MPa, the A_f and the martensite finish temperature (M_f) were estimated to be 157°C and 96°C, respectively.

The functional fatigue test rig was positioned in the thermostatic chamber that guaranteed a temperature of 80°C. The wire, which were axially loaded (600 MPa), was heated from 80°C by electrical pulse in order to recover the imposed deformation (3%). Then, the current source was switched off and the wire was cooled down to 80°C by natural air convection. The minimum and maximum strain values of each thermal cycle were plotted as a function of the number of cycles in Fig. 4. The wire withstood about 5000 cycles before failure. During cycling, the specimens accumulated 0.7% of irreversible deformation. It is worth noting that a plastic strain of 0.35% was accumulated in the first ten cycles, during the remaining thousands of cycles it accumulated only the left over 0.35%.

In order to demonstrate the possibility of using martensitic SMA for warm temperature actuators exploiting the HP-SME, it has been decided to apply a constant force to the specimens, because this is the simplest load condition. It is worth noting that, in most of real applications, springs are used as loading device. If a proper designed bias spring was applied instead of a weight, then the opposition load would have increased linearly with the displacement. Then the spring must be carefully chosen in order to overcome the threshold load to induce SIM.[24,25]

To conclude, Martensitic Nitinol micro-wires with A_f higher than RT were proven to be able to work as actuators in a warm temperature range, close to that of high-temperature SMAs, exploiting the HP-SME. They were loaded at 80°C above the superelastic plateau to induce SIM and thermally cycled between 80°C and 180°C. The fatigue life under 600 MPa was about 5000 cycles.

Acknowledgments

The authors would like to thanks E. Bassani of CNR IENI Lecco Unit for the technical assistance.

References

1. W. J. Buehler *et al.*, *J. Appl. Phys.* **34**, 1475 (1963).
2. K. Otsuka *et al.*, *Prog. Mater. Sci.* **50**, 511 (2005).
3. K. Otsuka and C. M. Wayman, *Shape Memory Materials* (Cambridge University Press, USA, 1998).
4. R. Casati *et al.*, *Scripta Materialia* **80**, 13 (2014).
5. M. Kohl *et al.*, *Sensor Actuators A* **70**, 104 (1998).
6. M. Kohl *et al.*, *J. Phys. IV* **C8**, 1187 192 (1995).
7. M. Kohl, *Shape Memory Actuators* (Springer-Verlag Berlin Heidelberg, USA, New York, 2004).
8. C. Grossmann *et al.*, *Metal Mater. Trans.* **40A**, 2530 (2009).
9. H. Funakubo *et al.*, *Robotica* **6**, 259 (1988).
10. R. Casati *et al.*, *Funct. Mater. Lett.* **5**, 1250009 (2012).
11. A. Tuissi *et al.*, *J. Mater. Eng. Perform.* **18**, 612 (2009).
12. J. San Juan *et al.*, *Nat. Nanotechnol.* **4**, 415 (2009).
13. X. Wang, *Scripta Materialia* **69**, 545 (2013).
14. C. Maletta *et al.*, *Smart Mater. Struct.* **21**, 112001 (2012).
15. T. Duerig *et al.*, *Mater. Sci. Eng. A* **273–275**, 149 (1999).
16. P. Wollants *et al.*, *Z. Metalkde* **70**, 113 (1979).
17. J. Frenzel *et al.*, *Acta Materialia* **58**, 3444 (2010).

18. J. Ma *et al.*, *Int. Mater. Rev.* **55**, 257 (2010).
19. S. Besseghini *et al.*, *Mater. Sci. Eng. A* **273-275**, 390 (1990).
20. G. S. Firstov *et al.*, *Scripta Materialia* **50**, 243 (2004).
21. C. A. Biffi *et al.*, *Intermetallics* **46C**, 4 (2014).
22. R. Casati *et al.*, *Procedia Eng.* **10**, 3423 (2011).
23. R. Casati *et al.*, *J. Mater. Eng. Perform.* **21**, 2633 (2012).
24. G. Scirè Mammano *et al.*, *Fract. Struct. Integrity* **21**, 25–33 (2013).
25. H. Funakubo (ed.), *Shape Memory Alloys* (Breach Science Publishers, New York, 1986).